

Time-resolved multispectral X-ray imaging with multi-channel Kirkpatrick-Baez microscope for plasma diagnostics at Shenguang-II laser facility

Shengzhen Yi (伊圣振)^{1,2,3}, Baozhong Mu (穆宝忠)^{1,2*}, Jingtao Zhu (朱京涛)^{1,2},
Xin Wang (王新)^{1,2}, Wenbin Li (李文斌)^{1,2}, Zhanshan Wang (王占山)^{1,2**},
Pengfei He (贺鹏飞)^{1,3}, Wei Wang (王伟)⁴, Zhiheng Fang (方智恒)⁴, and Sizu Fu (傅思祖)⁴

¹MOE Key Laboratory of Advanced Micro-Structured Materials, Shanghai 200092, China

²School of Physics Sciences and Engineering, Tongji University, Shanghai 200092, China

³School of Aerospace Engineering and Applied Mechanics, Tongji University, Shanghai 200092, China

⁴Shanghai Institute of Laser Plasma, CAEP, Shanghai 201800, China

*Corresponding author: mubz@tongji.edu.cn; **corresponding author: wangzs@tongji.edu.cn

Received March 5, 2014; accepted April 23, 2014; posted online July 18, 2014

A time-resolved multispectral X-ray imaging approach with new version of multi-channel Kirkpatrick-Baez (KB) microscope is developed for laser plasma diagnostics at the kilojoule-class Shenguang-II laser facility (SG-II). The microscope uses a total external reflection mirror in the sagittal direction and an array of multilayer mirrors in the tangential direction to obtain multiple individual high-resolution, high-throughput, and quasi-monochromatic X-ray images. The time evolution of the imploded target in multiple X-ray energy bands can be acquired when coupled with an X-ray streak camera. The experimental result of the time-resolved 2.5 and 3.0 keV dual-spectral self-emission imaging of the undoped CH shell target on SG-II is given.

OCIS codes: 340.7440, 310.6845, 230.4170, 340.7470.

doi: 10.3788/COL201412.083401.

Multispectral X-ray imaging of the implosion area is an important diagnostic approach in laser inertial confinement fusion research^[1]. It utilizes multiple quasi-monochromatic X-ray images to indicate temperature and density information of laser plasma through measurements of resonance line emission and continuum emission. The physics experiments to diagnose the dynamics of the undoped CH shell target at the kilojoule-class Shenguang-II (SG-II) laser facility in China make specific demands on the image intensity and spatial resolution of multispectral X-ray imaging approach. The temporal resolution can be realized by an X-ray streak camera in image plane, but it requires sufficient image intensity to obtain continuous time-resolved X-ray images. Meanwhile, the continuum X-ray emission from an undoped CH shell target is weak at the kilojoule-class SG-II laser facility, especially in the multi-keV X-ray range. A high spatial resolution of approximately 5 μm is necessary to resolve in detail the spatial localization of the imploded target's central core with only several tens of microns in diameter. In addition, a certain number of imaging channels are also required to couple with X-ray streak camera to obtain multiple X-ray energy bands (2.5 and 3.0 keV are needed for present experiments on SG-II).

The current multispectral X-ray imaging approaches include multimono-chromatic X-ray imager combining a pinhole array with a Bragg multilayer mirror (MMI)^[1-3], multi-channel bent crystals^[4,5], and four-channel Kirkpatrick-Baez (KB) microscope with single-layer-coated mirrors coupled to a plane crystal (i.e., a gated monochromatic X-ray microscope)^[6,7], which have been employed over the past decade. The simpler approach, MMI, uses an array of pinholes to improve the

signal-to-noise ratio of the pinhole imaging, and uses an X-ray multilayer mirror as the energy-dispersed element, but its spatial resolution is lower than 10 μm by the restriction of the pinhole diameter and diffraction effect together. The bent-crystal imaging being used has the advantages of high spectral resolution ($E/\Delta E = 10^3\text{-}10^4$) and a large aperture, but its best spatial resolution is also limited to the range of 6-10 μm due to the additional figure error when bending the crystal to the desired radius. The four-channel KB microscope can provide the spatial resolution of 3-5 μm within several hundred microns field of view, but it also has the disadvantage of low image brightness after the reflection of an energy-dispersed plane crystal. The above-mentioned approaches may not simultaneously meet both requirements of image intensity and spatial resolution on SG-II. The four-channel KB microscope with multilayer-coated mirrors is a feasible solution; however, with its image points arranged in a 2 \times 2 grid, only two images are available when used for time-resolved X-ray imaging with the streak camera, which cannot satisfy the requirement of the number of X-ray energy bands for future experiments.

In this letter, we propose a time-resolved multispectral X-ray imaging approach for the SG-II laser facility. This approach uses the new optical design of the multi-channel KB microscope (as shown in Fig. 1) to obtain high-throughput high-resolution X-ray images at multi-keV energy bands. It consists of a total reflection mirror (TRM) in the sagittal direction and an array of MMIs (M1-M4) in the tangential direction. The response to multiple X-ray energy bands is realized by the multilayers coated on the M1-M4. The image points A'1-A'4 are successively arranged along the same line to couple with

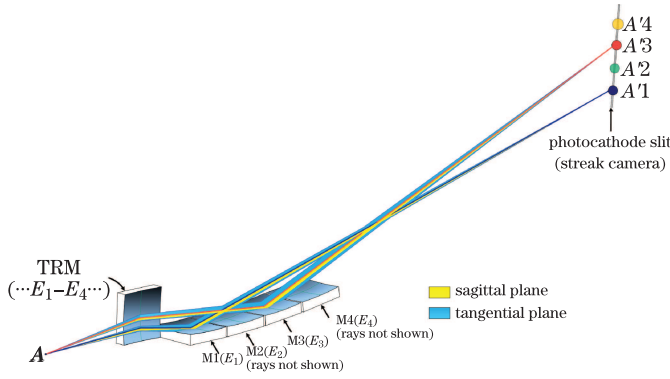


Fig. 1. (Color online) Schematic of the time-resolved multi-spectral X-ray imaging approach based on multi-channel multilayer KB microscope.

the photocathode slit of the streak camera, and time-resolved X-ray images along the longitudinal direction of the slit are obtained.

The imaging equation of each mirror in the tangential direction is given by

$$\frac{1}{u_i} + \frac{1}{v_i} = \frac{1}{u_i} + \frac{1}{M_i u_i} = \frac{1}{f_i} = \frac{2}{R_i \sin \theta_i}, \quad (1)$$

where u_i is the distance from the object to the center of the i th mirror, v_i is the distance from the center of the i th mirror to the image plane, M_i is the magnification, and R_i is the radius of curvature of the i th mirror. To overcome the astigmatism between tangential and sagittal directions, each mirror obeys the following equation:

$$u + v = u_1 + v_1 = \dots = u_4 + v_4, \quad (2)$$

where u is the distance from the object to the center of the TRM, and v is the distance from the center of the TRM to the image plane. Combining Eqs. (1) and (2), and with mirrors M1–M4 having the same curvature radius R_t , the relation between the sagittal mirror (TRM) and the tangential mirrors (M1–M4) is given by the following equation, where M is the magnification of the TRM.

$$\frac{(1+M)^2}{M} R \sin \theta = \frac{(1+M_i)^2}{M_i} R_t \sin \theta_i. \quad (3)$$

For the KB-type microscope, the X-ray image can be considered as independently formed in tangential and sagittal directions. Therefore, there are not particular requirements on the size and shape of the sagittal mirror (TRM) to accommodate four tangential mirrors. The four tangential mirrors faces the problem that the X-ray paths may be interrupted by each other. Here, we only analyse the relation between M1 and M2, but the optical parameters of the other three mirrors can also be determined in the same way. As shown in Fig. 2, the X-ray paths will not be mutually interrupted between mirrors M1 and M2 if the position of point B_2 is above the incident X-ray AB_1 and below the reflected X-ray $B_1A'1$. The concave spherical mirrors were considered as plane mirrors because of their small sagittal heights, i.e., of only a few microns. Thus, we can arrive at the following

relations:

$$m - \frac{d\theta_2}{2} > \frac{d\theta_1}{2} \quad (B_2 \text{ is above } AB_1), \quad (4)$$

$$m - \frac{d\theta_2}{2} < \frac{d\theta_1}{2} + 2 \cdot \Delta D \cdot \alpha_1 \quad (B_2 \text{ is below } B_1A'1), \quad (5)$$

where m is the vertical distance between the mirrors' centers O_1 and O_2 ; d is the length of mirrors M1 and M2; ΔD is the interval distance between points B_1 and B_2 ; α_1 is the grazing angle at the edge of M1. With the approximation of $\alpha_1 \approx \theta_1 \approx \theta_2$, Eqs. (4) and (5) can be simplified as

$$d\theta_1 < m < (d + 2\Delta D) \cdot \theta_1, \quad (6)$$

which gives the variation range of m as $2\Delta D \cdot \theta_1$. Its value is approximately $70 \mu\text{m}$ under the conditions of $\Delta D = 1 \text{ mm}$ and $\theta_1 = 2^\circ$, so the vertical distance is large enough to allow assembly and alignment of the instrument. Furthermore, four image points must be uniformly distributed on the slit of the streak camera to avoid overlapping each other; hence, the interval of two image points (ΔL illustrated in Fig. 2) must be accurately controlled. It can be deduced as

$$\begin{aligned} \Delta L &= L_2 - L_1 = \left(\frac{m}{u_2} + 2\theta_2 \right) v_2 + m - 2v_1\theta_1 \\ &= (M_2 + 1)m + 2(v_2\theta_2 - v_1\theta_1) < l/4, \end{aligned} \quad (7)$$

where L_1 is the vertical distance between image point $A'1$ and the axis of incident X-ray AO_1 ; L_2 is the vertical distance between image point $A'2$ and the axis of incident X-ray AO_2 ; l is the slit length of the streak camera, typically 15–30 mm. The spatial resolution of the KB microscope obviously decreases with the deviation in the object field because of serious off-axis aberration. For the approach of time-resolved multispectral X-ray imaging proposed in this study, the optical parameters of the multi-channel KB microscope must be appropriately selected to obey imaging Eq. (1) under the limits of Eqs. (6) and (7).

The TRM with small grazing angle θ utilizes the total external reflection to reflect the whole X-ray range E_1 – E_4 emitted from the imploded target (A). To realize the multispectral X-ray imaging, multilayers based on Bragg diffraction $2D_i \sin \theta_i = m\lambda_i$ are used as coatings on mirrors M1–M4 to work at different narrow-band X-ray ranges (E_1 – E_4), with the period thickness of the multilayers D_i defined by

$$D_i = \frac{m\lambda_i}{2 \sin \theta_i} = \frac{mhc}{2E_i \sin \theta_i}. \quad (8)$$

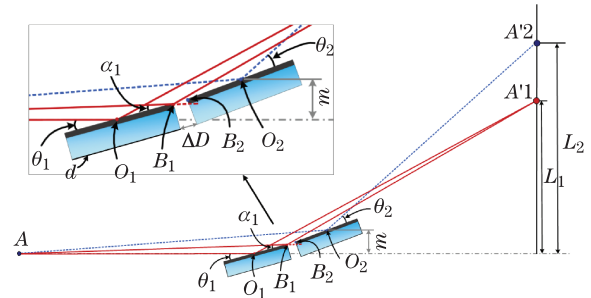


Fig. 2. (Color online) Schematic of X-ray paths between two mirrors (M1 and M2) in the tangential direction.

Table 1 shows the optical parameters of the multi-channel KB microscope designed for time-resolved 2.5–4.0 keV multispectral X-ray imaging at the SG-II facility. The mirror length d of 20 mm and approximately 3–4 times magnification were selected to obtain a sufficient solid angle and image intensity. Four image points were designed to distribute on the slit of the streak camera with the intervals of 5.60, 5.21, and 4.73 mm. The geometric solid angle of each channel changes in the range of 3.46×10^{-6} – 3.23×10^{-6} sr. The effective collecting efficiency of each channel is determined by the product of geometrical solid angle and the reflection efficiency of each mirror, and the spectral intensity of each channel at the image plane was determined by effective collecting efficiency and the magnification, which will be considered in the final analysis.

The response to given X-ray energies and grazing angles in Table 1 can be realized by the corresponding multilayers design. In this study, W/B₄C multilayers were used as TRM coating, and X-rays lower than 5 keV can be reflected by use of total external reflection. The multilayers coated on mirror M1–M4 include top Cr/C bilayers and bottom W/B₄C bilayers working at E_i and 8.05 keV, respectively. The reflectivities of these multilayers are shown in Fig. 3 with spectral bandwidth of approximately 200 eV (except the mirror TRM). The 8.05 keV X-rays can be generated by a common copper tube for performing alignment and assembly of the microscope in air (not in vacuum) since the long penetration depth compared to 2.5–4.0 keV soft X-rays. This will simplify the assembly process and ensure assembly accuracy. In physics experiments at the SG-II laser facility, 2.5–4.0 keV X-rays are reflected directly by the top Cr/C bilayers; hence the bottom W/B₄C bilayers will not reduce the X-ray throughput. The microscope performs well with the same optical path being used at 2.5–4.0 keV, and the image resolution is only slightly different from that at 8.05 keV owing to the X-ray diffraction effect. Furthermore, under the assumption that the self-emission X-ray spectrum is of the exponential form, the influence of 8.05 keV X-rays on lower soft X-ray images can be negligible.

At the present stage, we conducted 2.5 and 3.0 keV dual-spectral measurement of undoped CH shell target at the SG-II facility. Firstly, the 2.5 and 3.0 keV dual-channel KB microscope with the optical parameters of TRM, M3, and M4 as described in Table 1 was aligned by X-ray imaging experiment in the laboratory. The 600-mesh Au grid (41 μm period with approximately 6 μm linewidth measured by SEM) for use as the image calibration was backlit by a copper X-ray tube with the working voltage and current of 37.5 kV and 22 mA. The phosphor X-ray CCD (XDI-50 Photonic Science, UK) with 1392×1040 pixels and 6.45×6.45 (μm) pixel size was placed on the image plane. A coordinate grid was also placed before the X-ray CCD to stand for the slit position of streak camera. By successively aligning the mirror TRM in the tangential direction and the mirrors M3 and M4 in the sagittal direction, the final precise assembly was realized.

Figure 4(a) shows the X-ray image of the grid with the exposure time of 20 min after the assembly. The hole in the 600-mesh Au grid with a diameter of approxi-

mately 120 μm functions as a position reference from the object to the image. The interval of two image points measured by multiplying the number of pixels by 6.45 μm is well controlled at approximately 4.8 mm, which corresponds to the design value of 4.73 mm. The actual magnifications calibrated by the period of the grid were approximately $3.43 \times$ and $3.15 \times$ for the horizontal direction of $A'3$ and $A'4$, respectively. The spatial resolution in the vertical direction (imaging direction of streak camera) calibrated by “10%–90%” criterion^[8] is shown Fig. 4(b). Its value is in the range of 6–10 μm within 240 μm field of view. By adopting the concave spherical mirrors with lower figure error and surface roughness, the image resolution can be further improved to the level of existing KB microscopes.

At the SG-II laser facility, the microscope was used for self-emission imaging of an undoped CH shell target with a 260- μm diameter and 20- μm CH thickness. Eight synchronized laser beams (1 ns, 3ω , 200 J) directly illuminated eight quadrants of the target at the 45° angles with the equatorial plane. The slit of the streak camera (AXIS-PX, Axis Photonique Inc., Canada)^[9] was placed along the diameter direction of the target perpendicular to the equatorial plane. The 2.5 and 3.0 keV self-emission images of the imploded target with sufficient brightness

Table 1. Optical Parameters of the Multi-channel KB Microscope Designed for Time-resolved 2.5–4 keV Multispectral X-ray Imaging at the SG-II Laser Facility, the 2.5 and 3.0 keV Energy Bands are Used at Present Experiments

Optical Parameters	TRM	M1	M2	M3	M4
X-ray Energy, E_i (keV)	—	4.0	3.5	3.0	2.5
Grazing Angle, θ_i (deg.)	0.850	1.690	1.800	1.903	2.000
Curvature Radius, R, R_i (m)	29.0	13.5	13.5	13.5	13.5
Object Distance, u_i (mm)	204.1	248.1	270.1	292.1	314.1
Image Distance, v_i (mm)	1052.3	1008.3	986.3	964.3	942.3
Magnification, M_i	5.16	4.06	3.65	3.30	3.00
Image Interval, ΔL (mm)		5.60	5.21	4.73	

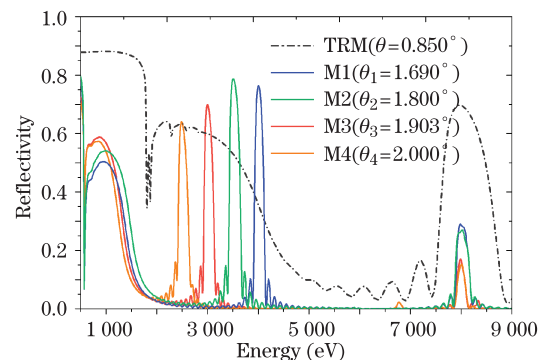


Fig. 3. (Color online) Reflectivities of the multilayers with spectral bandwidth of approximately 200 eV (except the mirror TRM) for use as the mirror coatings of multi-channel KB microscope.

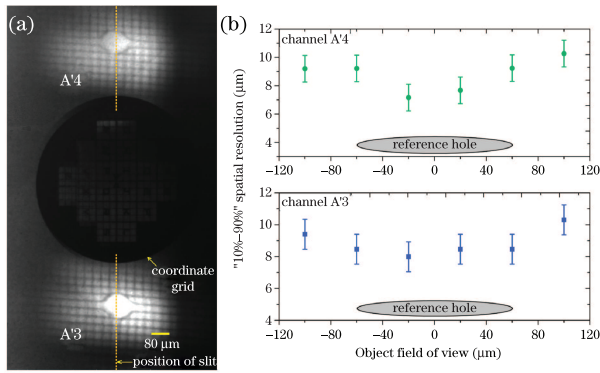


Fig. 4. (Color online) (a) Two 8 keV images ($A'3$ and $A'4$) obtained with the 2.5 and 3.0 keV dual-channel KB microscope. (b) The measured spatial resolutions based on “10%–90%” criterion in the vertical direction.

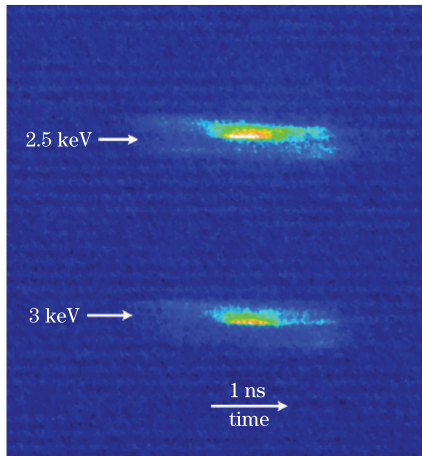


Fig. 5. (Color online) Time-resolved 2.5 and 3.0 keV self-emission images of the imploded CH shell target at the SG-II laser facility.

were formed by the mirrors TRM, M3, and M4, and then acquired by the streak camera, as shown in Fig. 5. The measured interval between two spots is approximately 4.8 mm, which corresponds to the value shown in Fig. 4(a). For each channel, the hotspot area with write color have higher intensity than outer area. The laser-irradiation nonuniformity of SG-II direct-drive experiments leads to the asymmetry in target compression. Meanwhile, 2.5 keV X-rays generated by bremsstrahlung radiation have more yields than 3.0 keV; therefore, the hotspot intensity at 2.5 keV is higher than 3.0 keV. Further comparison and analysis of spectral intensity can be conducted after considering the difference of two X-ray energies in effective

collecting efficiency, the magnification, and the spectral response of the streak camera.

In conclusion, we develop a time-resolved multispectral X-ray imaging approach with the new version of multi-channel KB microscope for laser plasma diagnostics at SG-II laser facility, and multiple individual high-resolution, high-throughput, and quasi-monochromatic X-ray images in the range of 2–4 keV can be obtained to indicate time evolution of the imploded plasma. This approach provides an effective diagnostics tool for X-ray self-emission imaging of the undoped target at the kilojoules-class laser facility. For the future experiments, the working X-ray range can be extended to greater than 4 keV through further optimizations such as reducing the grazing angle of the TRM or designing the multilayers of mirrors M1–M4 for higher X-ray energies. In addition, the diagnostic applications with more X-ray energy bands can be conducted by increasing the number of X-ray imaging channels.

This work was supported by the National Natural Science Foundation of China (Nos. 11305116 and 11105098), the National Key Technology Support Program (No. 2013BAK14B02), and the National “973” Program of China (No. 2011CB922203).

References

1. J. A. Koch, T. W. Barbee, Jr., N. Izumi, R. Tommasini, R. C. Mancini, L. A. Welsler, and F. J. Marshall, *Rev. Sci. Instrum.* **76**, 073708 (2005).
2. L. A. Welsler, R. C. Mancini, J. A. Koch, S. Dalhed, R. W. Lee, I. E. Golovkin, F. J. Marshall, J. Delettrez, and L. Klein, *Rev. Sci. Instrum.* **74**, 1951 (2003).
3. N. Izumi, T. W. Barbee, J. A. Koch, R. C. Mancini, and L. A. Welsler, *Rev. Sci. Instrum.* **77**, 083504 (2006).
4. I. Uschmann, K. Fujita, I. Niki, R. Butzbach, H. Nishimura, J. Funakura, M. Nakai, E. Förster, and K. Mima, *Appl. Opt.* **39**, 5865 (2000).
5. Y. Tian, W. Wang, C. Wang, X. Lu, C. Wang, Y. Leng, X. Liang, J. Liu, R. Li, and Z. Xu, *Chin. Opt. Lett.* **11**, 033501 (2013).
6. F. J. Marshall and J. A. Oertel, *Rev. Sci. Instrum.* **68**, 735 (1997).
7. S. Yi, B. Mu, X. Wang, J. Zhu, L. Jiang, Z. Wang, and P. He, *Chin. Opt. Lett.* **12**, 013401 (2014).
8. F. J. Marshall, M. M. Allen, and J. P. Knauer, *Phys. Plasmas* **5**, 1118 (1998).
9. Axis Photonique Inc., “AXIS-PX: Ultrafast X-ray Streak Camera,” <http://www.axis-photon.com/en/AXIS-PX.shtml>, (April 20, 2014).